Deriving Atmospheric Temperature of the Tropopause Region–Upper Troposphere by Combining Information from GPS Radio Occultation Refractivity and High-Spectral-Resolution Infrared Radiance Measurements

EVA E. BORBAS

Cooperative Institute for Meteorological Satellite Studies, University of Wisconsin—Madison, Madison, Wisconsin

W. PAUL MENZEL

NOAA/NESDIS Office of Research and Applications, Madison, Wisconsin

ELISABETH WEISZ

Cooperative Institute for Meteorological Satellite Studies, University of Wisconsin—Madison, Madison, Wisconsin

DEZSO DEVENYI

Cooperative Institute for Research in Environmental Sciences, University of Colorado, Boulder, Colorado

(Manuscript received 10 January 2007, in final form 4 January 2008)

ABSTRACT

Global positioning system radio occultation (GPS/RO) measurements from the Challenging Minisatellite Payload (CHAMP) and Satelite de Aplicaciones Cientificas-C (SAC-C) satellites are used to improve tropospheric profile retrievals derived from the *Aqua* platform high-spectral-resolution Atmospheric Infrared Sounder (AIRS) and broadband Advanced Microwave Sounding Unit (AMSU) measurements under clear-sky conditions. This paper compares temperature retrievals from combined AIRS, AMSU, and CHAMP/SAC-C measurements using different techniques: 1) a principal component statistical regression using coefficients established between real (and in a few cases calculated) measurements and radiosonde atmospheric profiles; and 2) a Bayesian estimation method applied to AIRS plus AMSU temperature retrievals and GPS/RO temperature profiles. The Bayesian estimation method was also applied to GPS/RO data and the AIRS Science Team operational level-2 (version 4.0) temperature products for comparison. In this study, including GPS/RO data in the tropopause region produces the largest improvement in AIRS–AMSU temperature retrievals—about 0.5 K between 100 and 300 hPa. GPS/RO data are found to provide valuable upper-tropospheric information that improves the profile retrievals from AIRS and AMSU.

1. Introduction

The combination of active remote sensed global positioning system (GPS) data and passive high–spectral resolution infrared (IR) radiometric measurements [like Atmospheric Infrared Sounder (AIRS)] is studied to improve the quality of the atmospheric temperature retrievals over those achievable from either system alone. Improved retrievals are considered likely because the two systems have complementary characteristics (Collard and Healy 2003), especially around the tropopause region: the GPS radio occultation (GPS/RO) system provides good absolute accuracy (0.15% in refractivity) near the tropopause with very good vertical resolution (100 m) but poorer horizontal resolution (500 km), while the AIRS IR sounding system has high horizontal (13.5 km at nadir) but poorer vertical resolution (1 km for temperature and 2 km for moisture at the tropopause and below; see Aumann et al. 2003; http://www-airs.jpl.nasa.gov/Data/GetAIRSdata/CoreProducts/). In an earlier study, Borbas et al. (2003) showed that adding GPS/RO measurements to Ad-

Corresponding author address: Eva E. Borbas, CIMSS/UW-Madison, 1225 W. Dayton St., Madison, WI 53706.
E-mail: eva.borbas@ssec.wisc.edu

DOI: 10.1175/2008JAMC1687.1

vanced Television and Infrared Observation Satellite (TIROS) Operational Vertical Sounder (ATOVS) retrievals produced improved atmospheric temperature and moisture profiles.

Using measurements from polar orbiting infrared and microwave (MW) sounders, radiometric techniques infer temperature and moisture profiles in the lower and upper troposphere with limited vertical resolution, since the measurements are highly correlated. In addition, in the tropopause region, where temperature does not change appreciably with height, radiometric techniques are challenged to distinguish the tropopause altitude. GPS radio occultation measurements can provide refractivity profiles with high accuracy around the tropopause and in the stratosphere that are related to temperature and moisture (Ware et al. 1996; Rocken et al. 1997). Improved temperature and moisture profile retrievals are thought to be possible by combining data from these two complementary systems. More recently, information from AIRS and GPS/RO measurements from the Challenging Minisatellite Payload (CHAMP), Satelite de Aplicaciones Cientificas-C (SAC-C), and later Constellation Observing System for Meteorology, Ionosphere and Climate (COSMIC) is being assimilated in numerical weather prediction (NWP) models at operational NWP centers (e.g., the European Centre for Medium-Range Weather Forecasts and the Joint Center for Satellite Data Assimilation) with positive impact in the upper troposphere and stratosphere (Cucurull et al. 2006; Healy and Thepaut 2006; Kuo et al. 2000; Liu et al. 2007).

The GPS/RO is an active limb sounding system. The current radio-based satellite navigation system, the global positioning system (see Hofmann-Wellenhof et al. 2004 for GPS theory) operated by the United States, has 24 satellites that transmit radio signals on two frequencies continuously. In the near future (2010–11), the Russian Global Navigation Satellite System (GLONASS) will be restored and the European Galileo system will become operational providing increased opportunities for more occultations. In a GPS/RO system the receiver is generally located on a low earth orbiting (LEO) satellite. An occultation occurs whenever a GPS (transmitter) satellite rises or sets over the earth and the transmission path traverses the earth's atmospheric limb. The ray path through the atmosphere is refracted according to Snell's law. Knowing the exact locations of the receiving and transmitting satellites allows the refractive index (or refractivity) of the atmospheric layer through which the ray passes to be derived. The movement of the two satellites produces a vertical profile of refractivity. With 24 GPS transmitter satellites, approximately 500 occultations globally are received by an LEO satellite such as CHAMP or SAC-C. With the launch of the six LEO spacecraft for the new U.S. and Taiwan COSMIC mission (Rocken et al. 2004) in April 2006, a massive increase in the number of GPS/RO measurements (about 2500 occultations per day) occurred.

Radiances from AIRS, a high-spectral-resolution infrared sounder, along with brightness temperatures (BTs) from Advanced Microwave Sounding Unit-A (AMSU), a microwave sounder, were combined with the GPS/RO measurements in this study. The AIRS and AMSU instruments were launched on the National Aeronautics and Space Administration (NASA) Earth Observing System (EOS) *Aqua* satellite in May 2002. More information about the AIRS instrument and measurements can be found in Aumann et al. (2003) or on the Web (http://airs.jpl.nasa.gov/). The operational AIRS level 2 (L2) V4.0 retrievals are described in Susskind et al. (2006).

This paper combines GPS/RO and AIRS–AMSU measurements in a statistical study to better define the tropopause location and temperature. Section 2 provides a summary of the data used in this study. Section 3 describes the retrieval methods. Section 4 discusses the cloud screening approach and the AIRS spectral channel selection. Results are presented in section 5 and validation at the Atmospheric Radiation Measurement Program (ARM; Ackerman and Stokes 2003; Stokes and Schwartz 1994) sites is in section 6. Conclusions follow in section 7.

2. The data

AIRS, AMSU, and GPS/RO (from both CHAMP and SAC-C satellites) measurements and radiosonde observations (raob) were collected between September 2002 and December 2005. Raobs were used for both training algorithms and subsequent validation. GPS/RO data were extracted at 200-m vertical resolution at altitudes between 8 and 26 km. Over 380 000 AIRS-raob collocations from the National Centers for Environmental Prediction (NCEP) quality controlled final observation data files (PREPQC) and over 50 000 SAC-C (September 2002–January 2005) and 140 000 CHAMP (September 2002–December 2005) occultations between 8 and 26 km were collocated from the NASA/Jet Propulsion Laboratory (JPL) Genesis Web site for this study. The criteria for collocation were a time separation of <3 h and distance separation of <300 km. AIRS measurements were assumed to be made at nadir and raobs were assumed to have no horizontal drift. Since the GPS/RO measurements have

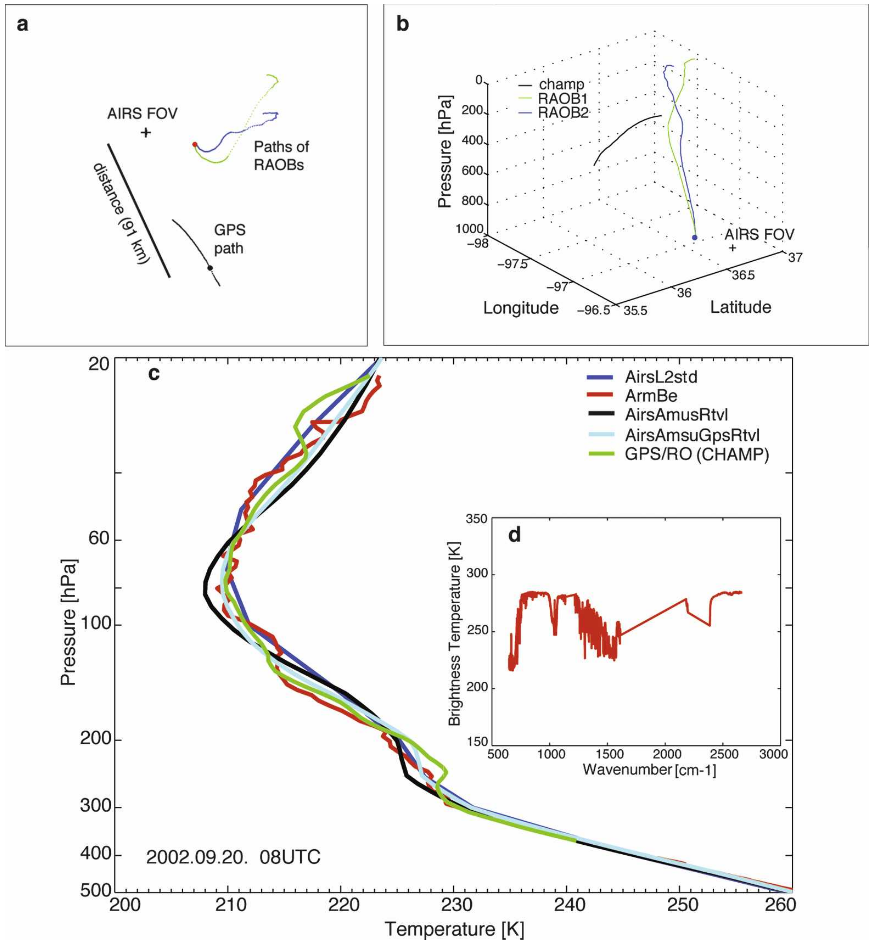

FIG. 1. An example of AIRS–AMSU, GPS/RO data and best estimate profile collocation over the SGP site. (a),(b) The locations–tracks of the different measurements. (c) The temperature retrievals from different sources: AIRS L2 product (AirsL2std; blue), the ARM best estimate profile (ArmBe; red), the AIRS–AMSU PC statistical regression temperature retrieval without GPS/RO data (AirsAmsuRtvl; black) and with GPS/RO data (AirsAmsuGpsRtvl; light blue), and the GPS/RO temperature profile (GPS/RO; green). (d) Observed AIRS BTs.

considerable horizontal extent (as much as 500 km or more) and this study focuses on the tropopause region, the location of the occultations was considered to be at the tangent point at 11 km and the GPS/RO profiles were also assumed to be vertical. An illustration of the horizontal shift of raob measurements and GPS/RO occultations can be seen in Figs. 1a,b.

These data yielded 5336 AIRS–AMSU–GPS–raob collocations (top panel of Fig. 2). After testing for clear-sky conditions (see section 4 for more details), 973 collocations remained (bottom panel of Fig. 2); of these, 841 include operational AIRS collection 4 products [with quality flag (Qual_temp_profile_top) equal to 0]. To establish a training dataset along with a test dataset, every fifth collocation was placed in the test dataset and the remaining 80% were used as a training dataset for the retrieval methods described below.

3. Retrieval methods

Several retrieval approaches were tried on the clear-sky dataset containing 841 collocated samples. To show the effect of the high vertical resolution GPS/RO data, the statistics were calculated for 101 pressure levels instead of 1 or 2 km layers as is more common (Divakarla et al. 2006; Susskind et al. 2006; Tobin et al. 2006; Weisz et al. 2007; Wu et al. 2005). Using 101 levels revealed details that are suppressed when using just layers. Bias and RMS differences were computed between the retrievals and collocated (PREPQC) radiosonde profiles in the test dataset.

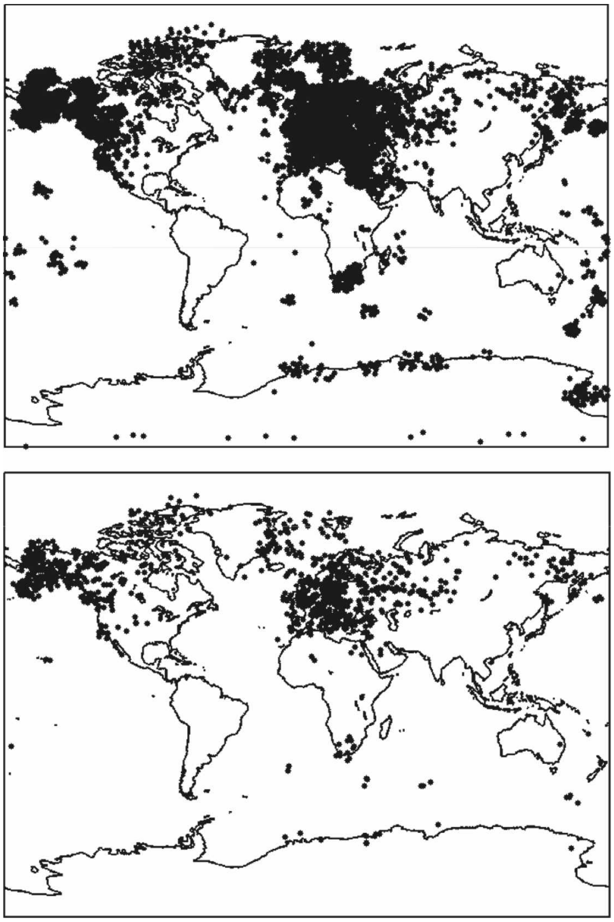

FIG. 2. AIRS, AMSU, GPS/RO, and raob collocations under (top) all (5336 collocations) and (bottom) clear-sky (973 collocations) conditions.

a. PC statistical regression method

A principal component (PC) statistical regression (Smith and Woolf 1976; Huang and Antonelli 2001; Goldberg et al. 2003) was used on the AIRS–AMSU radiances and GPS/RO refractivities. The PC statistical regression is a least squares regression that uses principal components (eigenvectors) for predictors (see Goldberg et al. 2003). The single field of view (FOV) University of Wisconsin—Madison International Moderate Resolution Imaging Spectroradiometer (MODIS)/AIRS Processing Package (IMAPP) (Huang et al. 2004; Weisz et al. 2003, 2007) was modified to accommodate the addition of AMSU and GPS/RO data (referred to as the AIRS–AMSU–GPS/RO PC statistical regression method). In the statistical regression method, a linear relationship is assumed between the atmospheric state vector [$\mathbf{X}$ (nl, ns), deviation from the mean value] and the measurements [$\mathbf{Y}$ (ns, nd), deviation from the mean value]: $\mathbf{X} = \mathbf{C}\mathbf{Y}^{\mathrm{T}}$, where $\mathbf{C}$ (nl, nd) is the matrix of the regression coefficients, nl stands for the number of levels, ns is the number of samples in the training dataset, and nd is the dimension of the measurements (the number of independent pieces of information, which is the sum of the number of AIRS and AMSU channels plus the number of GPS levels in our study). In the PC statistical regression the following relationship is used instead:

$$\mathbf{X} = \mathbf{C}\mathbf{A}^{\mathrm{T}}, \tag{1}$$

where the dimension of $\mathbf{C}$ is now (nl, npc) and

$$\mathbf{A} = \mathbf{Y}\mathbf{U}. \tag{2}$$

The $\mathbf{A}$ (ns, npc) stands for the matrix of compressed measurements, which are commonly called projection coefficients or PC scores, T stands for the matrix transposition, npc is the number of eigenvectors of the measurements, and $\mathbf{U}$ (nd, npc) is the matrix containing the first few (npc) eigenvectors of the covariance matrix of $\mathbf{Y}$. In the least squares solution, the minimization of $\Sigma(\mathbf{X} - \mathbf{C}\mathbf{A}^{\mathrm{T}})^2$ results in the regression coefficients $\mathbf{C}$:

$$\mathbf{C} = \mathbf{X}_{\mathrm{tr}}\mathbf{A}_{\mathrm{tr}}(\mathbf{A}_{\mathrm{tr}}^{\mathrm{T}}\mathbf{A}_{\mathrm{tr}})^{-1}, \tag{3}$$

where tr refers to training data and -1 stands for the matrix inversion. The atmospheric state vector ($\mathbf{X}_{\mathrm{tr}}$) includes temperature and moisture profiles at 101 pressure levels from 0.005 to 1100 hPa and the surface pressure of collocated radiosonde measurements, while the measurements ($\mathbf{Y}$) in $\mathbf{A}_{\mathrm{tr}}$ include the collocated AIRS radiances, the atmospheric-sensitive (channels 6–14) AMSU-A BTs, and GPS/RO refractivity profiles. Then the atmospheric parameters ($\mathbf{X}_{\mathrm{retr}}$) are retrieved according to

$$\mathbf{X}_{\mathrm{retr}} = \mathbf{C}\mathbf{A}_{\mathrm{obs}}^{\mathrm{T}}, \tag{4}$$

where $\mathbf{A}_{\mathrm{obs}}$ is the matrix of the compressed observations of the test data.

Earlier studies on AIRS data showed that 30 eigenvectors calculated from the covariance matrix of AIRS radiances simulated from the training dataset were sufficient for retrieval purposes. In this study we also used 30 eigenvectors (principal components) associated with the largest eigenvalues to reduce the dimension of the regression problem and to stabilize the inverse of the predictor matrix ($\mathbf{A}$) in Eq. (3). The same 1688 National Oceanic and Atmospheric Administration/National Environmental Satellite, Data, and Information Service (NOAA/NESDIS) preselected AIRS channels were used in this study as are used in the AIRS IMAPP software. Measurements from atmospheric-sensitive AMSU-A channels (6–14) were also used. GPS/RO refractivity profiles with 200-m vertical resolution between only 8- and 26-km height were used. The IMAPP algorithm (Weisz et al. 2007) includes a brightness temperature (6 categories) and a scanning angle classification (with 11 categories); these classifications were not included for the real data coefficient determination as the collocated training dataset was too small (650 profiles).

Temperature retrievals with and without GPS/RO refractivity data were compared to 164 (PREPQC) radiosonde profiles.

b. *PC statistical regression method using calculated measurements for training*

In our earlier study, the PC regression coefficients were generated from simulated AIRS, AMSU, and GPS/RO data to study the influence of random noise. The so-called SeeBor (Seemann–Borbas) training data (Borbas et al. 2005) were used; this dataset includes over 12 000 clear-sky atmospheric temperature, moisture, and ozone profiles assigned with realistic surface properties (e.g., emissivity and skin temperature).

The stand-alone radiative transfer algorithm (SARTA) forward model (Strow et al. 2003) V1.06 was used to calculate AIRS radiances from the training dataset. Prelaunch determinations of noise equivalent delta temperatures (NEDTs) for the AIRS and AMSU-A channels were used to generate Gaussian random noise. AMSU temperatures were calculated using a microwave adaptation of pressure-layer optical depth/pressure-layer fast algorithm for atmospheric transmittances (PLOD/PFAAST) (Hannon et al. 1996) based on line-by-line calculations with the Millimeter-wave Propagation Model (MPM) (Liebe et al. 1993). GPS/RO refractivity profiles between 8 and 26 km with 200-m vertical resolution were calculated using the approach described in Borbas et al. (2003); this approach is based on the Healy and Eyre (2000) method and the Kursinski et al. (1997) error estimations. Regression coefficients were generated for calculated AIRS radiances, AMSU brightness temperatures, and GPS/RO refractivity profiles against the temperature, moisture, and ozone profiles and surface parameters like surface temperature, surface pressure, IR surface emissivity, and reflectivity.

Inspection of real and synthetic regression coefficients in combined AIRS–AMSU–GPS/RO PC statistical regressions showed that synthetic coefficients did not produce better results. Thus the study presented in section 5 used regression coefficients established with real measurements. In section 6, the ARM best estimate comparisons used synthetic coefficients established with calculated measurements to increase the training sample size.

c. *Combined temperature retrievals using Bayesian estimation*

The Bayesian estimation (see, e.g., Lorenc 1986) was also used to combine the already retrieved AIRS–AMSU and GPS/RO temperature profiles. This method allows us to investigate the impact of GPS/RO data on the operational AIRS L2 products.

In the Bayesian estimation, minimization of the following cost function (J),

$$J(\mathbf{t}) = \frac{1}{2}(\mathbf{t}-\mathbf{t}_1)^{\mathrm{T}}\mathbf{A}^{-1}(\mathbf{t}-\mathbf{t}_1) + \frac{1}{2}(\mathbf{t}-\mathbf{t}_2)^{-1}\mathbf{B}^{-1}(\mathbf{t}-\mathbf{t}_2), \tag{5}$$

yields the combined temperature profiles ($\mathbf{t}$) from AIRS–AMSU temperature profile retrievals ($\mathbf{t}_1$) and the operational GPS/RO temperature profiles ($\mathbf{t}_2$). GPS/RO temperature profiles were previously interpolated to the 101 pressure levels. Since only GPS/RO data between 8 and 26 km were used, the interpolation yields GPS/RO data at pressure levels between 23 and 286 hPa.

In Eq. (5), $\mathbf{A}$ (101, 101) and $\mathbf{B}$ (36, 36) are the error covariance matrices of combined AIRS–AMSU temperature profile retrievals ($\mathbf{t}_1$) and GPS/RO temperature profiles ($\mathbf{t}_2$), respectively. Both $\mathbf{A}$ and $\mathbf{B}$ (both symmetric and positive definite) are computed from the training dataset including collocated radiosonde profiles.

Minimizing the cost function gives the following:

$$\mathbf{A}^{-1}(\mathbf{t}-\mathbf{t}_1) + \mathbf{B}^{-1}(\mathbf{t}-\mathbf{t}_2) = 0, \tag{6}$$

and then the combined temperature profile can be calculated according to

$$\mathbf{t} = (\mathbf{A}^{-1}\mathbf{t}_1 + \mathbf{B}^{-1}\mathbf{t}_2)(\mathbf{A}^{-1} + \mathbf{B}^{-1})^{-1}. \tag{7}$$

Bayesian estimation was used to combine the GPS/RO temperature profiles with the AIRS–AMSU PC statistical regression temperature retrievals and also with the operational AIRS L2 support temperature retrieval products (referred to as the operational AIRS L2 product; Aumann et al. 2005). The operational AIRS L2 products are derived by a physical inversion scheme with 100 pressure levels using cloud-cleared radiances on the AMSU footprint (which is covered by a 3 × 3 matrix of AIRS footprints); details regarding the operational AIRS L2 algorithm can be found in Susskind et al. (2003, 2006).

4. Cloud masking and reducing the number of channels

Building upon several cloud masks (Ackerman et al. 1998), the following criteria were used to detect the

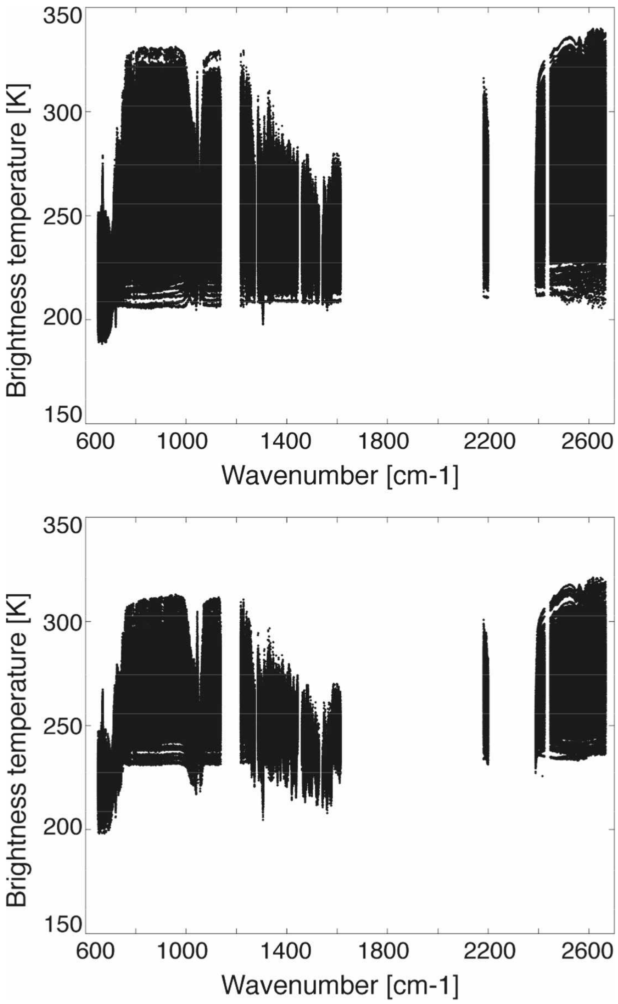

FIG. 3. Observed AIRS BTs at 1688 selected channels under (top) all and (bottom) clear-sky conditions.

presence of clouds. Clouds were assumed when measured spectra had 10 or more channels with brightness temperature differences greater than 7 K with respect to brightness temperatures calculated from collocated raob profiles. The effect of cloud screening is illustrated in Fig. 3.

In addition to the cloud mask, we also looked at the number of channels to use in our study. Direct assimilation of radiances in the NWP model requires some channel selection. We also create subsets of the available channels to study NWP-like information content. The AIRS–AMSU PC statistical regression retrievals from 1688 AIRS channels have been compared to AIRS–AMSU PC statistical regression retrievals from 394 optimally selected channels (see Fig. 4) that are used in an AIRS physical retrieval method (Wu et al. 2005). Using 1688 channels in the PC regression method improves temperature retrievals below 300 hPa

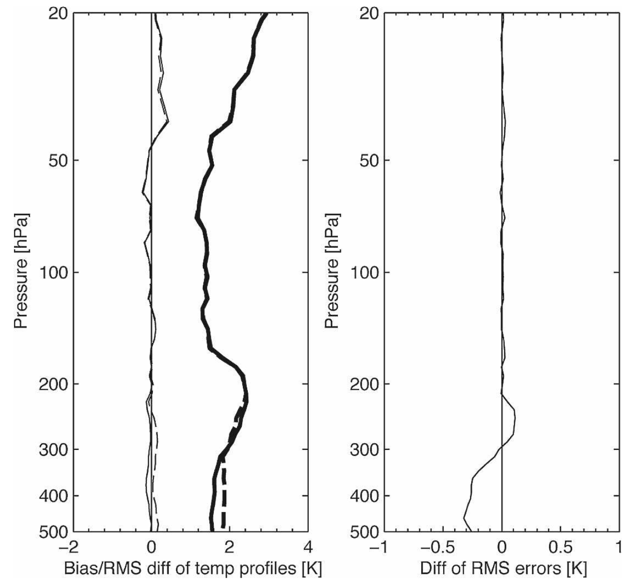

FIG. 4. Effect of channel selection on AIRS–AMSU statistical retrievals: (left) bias (thin) and RMS (thick) differences of AIRS–AMSU retrieval using 1688 (solid) vs 394 (dashed) AIRS channels against raob data; (right) difference of the two RMS profiles (1688 channels minus 394 channels).

by 0.15 K. For tropopause studies, 394 channels would be adequate.

5. Results

a. The PCA statistical regression retrieval method

Bias and RMS differences of the AIRS–AMSU–GPS/RO (GPS refers to CHAMP or SAC-C depending on the data collocation) combined PC statistical regression retrievals (solid), AIRS–AMSU retrievals (dash), and GPS/RO retrievals (dot) against radiosonde measurements are shown in Fig. 5, where the black solid line on the right-hand panel represents the differences in RMS (positive values indicate positive impact using GPS/RO data in the retrieval method). AIRS–AMSU only and GPS/RO only have comparable RMS differences w.r.t. raobs, and the combination shows a positive impact between 100 and 300 hPa with two peaks: one around 200 hPa with a maximum of 0.5 K and one around 270 hPa with a maximum of 0.7 K. AIRS–AMSU–GPS/RO retrievals outperform GPS/RO-only and AIRS–AMSU-only retrievals because of the complementary nature of these measurements.

b. Results using a Bayesian technique to combine AIRS–AMSU and GPS/RO temperature profiles

The impact of GPS/RO data on AIRS–AMSU retrievals was also investigated using the Bayesian esti-

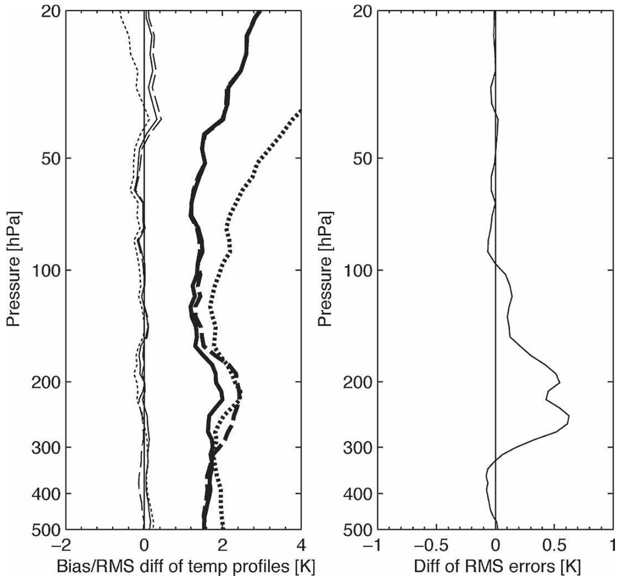

FIG. 5. (left) Comparison of only GPS/RO (dotted) and AIRS–AMSU PC statistical regression retrievals with (solid) and without (dashed) GPS/RO data with radiosonde measurements. Bias (thin) and RMS (thick) differences are shown. (right) Difference between the two RMS profiles (without GPS/RO minus with GPS/RO).

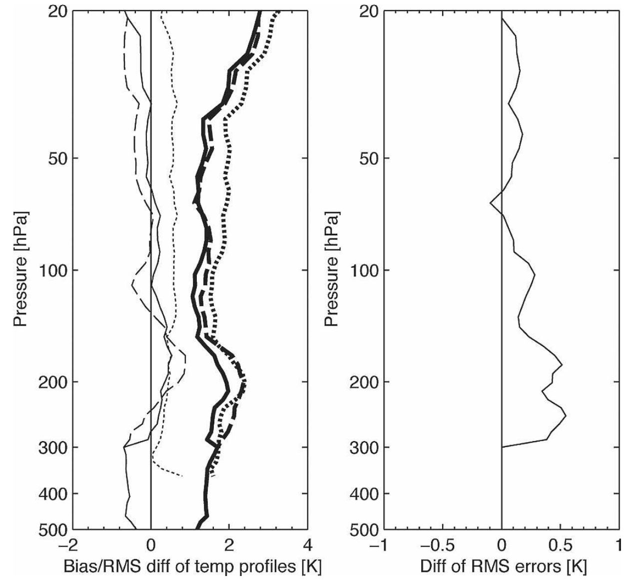

FIG. 6. (left) Bias (thin) and RMS (thick) differences of operational version-4 AIRS L2 products (dashed), GPS/RO temperature profiles (dotted), and the combination temperature retrievals (solid) using the Bayesian estimation method in comparison with raob measurements. (right) Difference of the original AIRS L2 product and combined profile RMS differences.

mation (discussed in section 3c) to combine the retrievals and GPS/RO profiles. This approach is independent of the PC statistical regression retrieval technique and allows us to investigate the impact of GPS/RO data on the operational AIRS L2 products that are derived by an advanced physical regression retrieval scheme. The Bayesian estimation method was applied for each level where both AIRS–AMSU and GPS/RO profiles were found. The operational AIRS L2 products were selected from the 100 pressure level support products. Figure 6 shows the combined operational AIRS L2 and GPS/RO products; results are improved by 0.5 K at 250 and 180 hPa when compared with radiosonde measurements and GPS/RO has a positive effect almost everywhere where it was included (between 20 and 300 hPa).

Figure 7 shows the outcome of applying the Bayesian estimation method to the AIRS–AMSU PC statistical regression profiles. Similar results are shown: the GPS/RO data improved the AIRS–AMSU PC statistical regression retrievals, but now the maximum improvement is 0.7 K around 250 hPa. The improvement is larger for the PC statistical retrievals because these retrievals show larger errors with respect to the radiosonde than the operational AIRS L2 retrievals.

In Fig. 8, application of the Bayesian estimation method on AIRS–AMSU statistical retrievals and GPS/RO data is compared with the AIRS–AMSU–GPS/RO PC statistical retrievals on the same test dataset. The two methods produce very similar results—the two approaches are not distinguishable in this study.

In Fig. 9 the AIRS–AMSU PC statistical regression retrievals combined with GPS/RO via the Bayesian estimation method are compared with the operational AIRS L2 products combined with GPS/RO via the Bayesian estimation method; note that between 300 and 500 hPa only AIRS–AMSU data are used. Using the Bayesian estimation method on the operational AIRS L2 temperature products and GPS/RO profiles produces RMS differences w.r.t. raobs that are 0.2 K smaller than when used on AIRS–AMSU PC regression retrievals and GPS/RO data. This outcome is likely due to the higher quality of the operational AIRS L2 products as compared to the AIRS–AMSU PC statistical regression retrievals.

6. Validation over the SGP and NSA ARM sites

The AIRS–AMSU plus GPS/RO results were validated against the "best estimate of the atmosphere" developed to validate the operational AIRS L2 products over the ARM program sites. Best estimate data include atmospheric vertical profiles of pressure, temperature, moisture, and surface parameters. These profiles of the atmospheric state are an ensemble of tem-

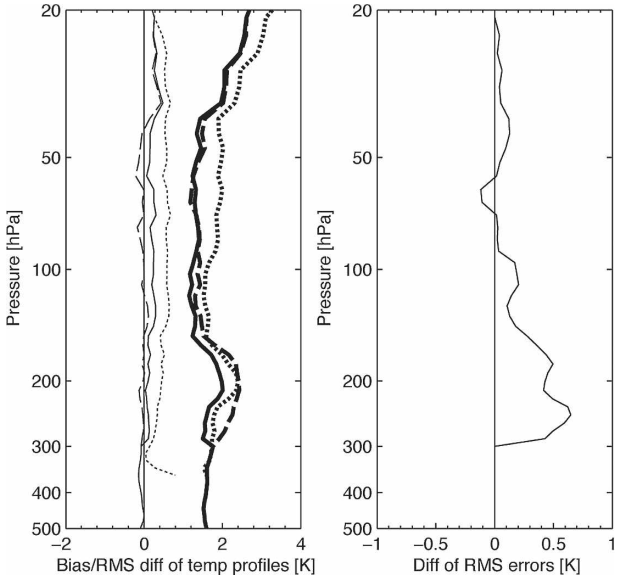

FIG. 7. (left) Bias (thin) and RMS (thick) differences of AIRS–AMSU PC statistical retrievals (dashed), GPS/RO (dotted), and the combination (solid) by the Bayesian estimation method compared against raob measurements. (right) Difference of AIRS–AMSU PC statistical retrieval and the combined profile RMS differences.

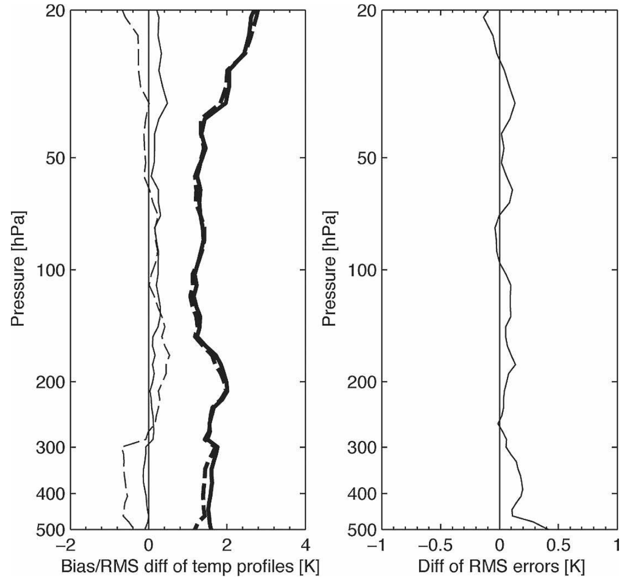

FIG. 9. Comparison of operational AIRS L2 (dashed) and PC statistical regression AIRS–AMSU (solid) retrievals combined with GPS/RO retrievals via Bayesian estimation method. Thin lines stand for the bias and thick lines represent the RMS differences. (right) Difference of the RMS profiles (RMS of combined GPS/RO and PC statistical regression retrievals minus RMS of combined GPS/RO and AIRS L2 products).

perature and moisture profiles created from two radiosondes launched within 2 h of the *Aqua* satellite overpass times (see Tobin et al. 2006). Datasets from the Southern Great Plains (SGP) central facility site in Oklahoma and the North Slope of Alaska (NSA) site near Barrow, Alaska, were used—over 800 samples at the SGP site and about 400 collocations at the NSA site. GPS/RO data between 8 and 26 km with 200-m vertical resolution were used. The clear-sky cases were selected manually by looking at the observed AIRS brightness temperature spectra and the retrieved temperature profiles. Figure 1 shows an example case over the SGP site and illustrates the nature of these comparisons. Neither radiosonde nor GPS/RO measurements are vertical; Fig. 1a illustrates the map of the two radiosondes, which were used to create the best estimate profile, the track of the GPS/RO measurement, and the location of the AIRS FOV. Figure 1b gives a three-dimensional illustration of the location of the radiosonde and GPS/RO measurements. Figure 1c illustrates all available temperature profiles, including the operational AIRS L2 retrieval, the best estimate profile, AIRS–AMSU PC statistical regression retrievals with and without GPS/RO data, and the GPS/RO temperature profile. AIRS observed brightness temperatures for this case are plotted in Fig. 1d.

Clear-sky GPS/RO collocation yielded 26 cases; given the low number of clear-sky collocations, the SGP and NSA sites were considered together in calculating the statistics. To benefit from a larger training

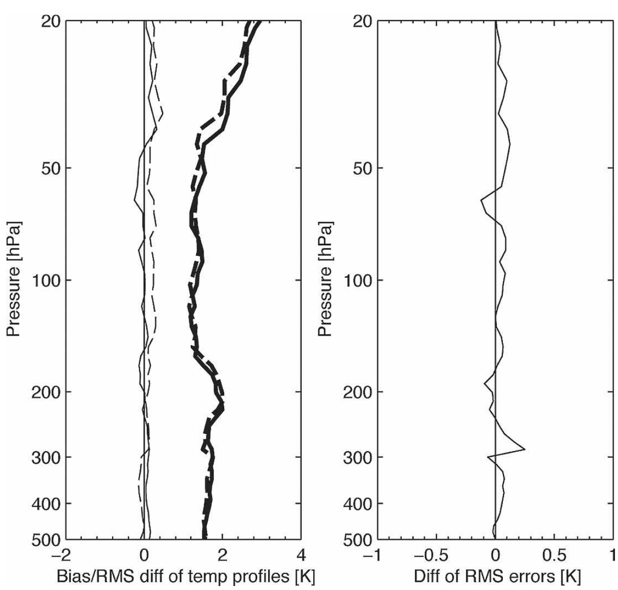

FIG. 8. (left) Comparison of results using PC statistical regression (solid) vs Bayesian estimation method (dashed). Thin lines stand for the bias and thick lines represent the RMS differences. (right) Difference of the RMS profiles (PC statistical regression minus Bayesian estimation method).

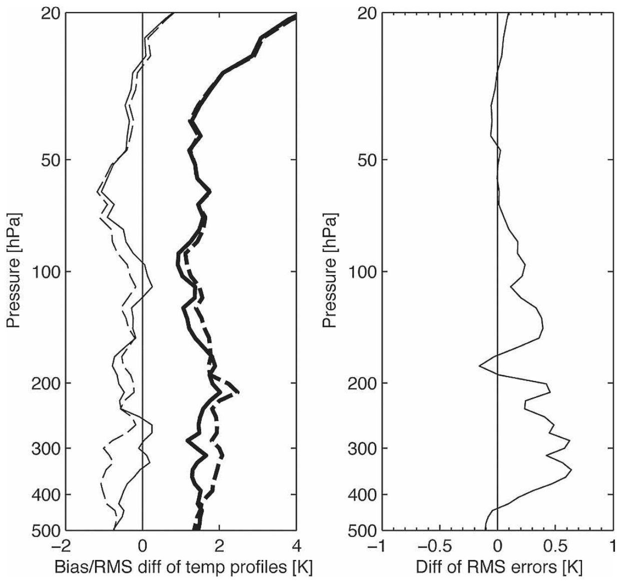

FIG. 10. Validation of the AIRS–AMSU PC statistical temperature retrievals without (dashed) and with (solid) GPS/RO data with the best estimate profiles at the SGP and NSA ARM sites. (right) The difference of the two RMS profiles as the impact of using GPS/RO data in the retrievals. Positive values indicate improvements. Synthetic coefficients were used in the regression retrieval.

sample size, PC statistical regression retrievals in the ARM site study used synthetic regression coefficients that have global applicability. Figure 10 shows the bias and RMS differences between AIRS–AMSU PC statistical regression temperature retrievals with and without GPS/RO data and the best estimate profiles. A positive impact of 0.5 K between 100 and 450 hPa is consistent with the earlier study using the PREPQC dataset.

Figure 11 shows two example collocations that demonstrate positive and neutral impacts of GPS/RO data on the temperature retrieval. Figure 11a shows temperature retrievals (including combined AIRS–AMSU PC statistical regression retrieval and operational AIRS L2 products) that do not capture the tropopause as well as the GPS/RO temperature and ARM best estimate profiles. Figure 11b shows an example where adding the GPS/RO data improves the PC statistical temperature retrieval at the tropopause.

7. Conclusions

In this paper, we show that the AIRS–AMSU temperature retrievals have the largest improvement from the inclusion of GPS/RO in the tropopause region—about 0.5 K between 100 and 300 hPa. GPS/RO data are found to provide valuable upper-tropospheric information that improves the AIRS–AMSU profile retrieval. The practical consequence of improved retrievals in clear skies from the combination of the information contained in AIRS radiances and GPS refractivities is that numerical weather prediction models can be expected to show positive forecast impact from the assimilation of both that exceeds the impact achieved from assimilating either one alone.

We used combined temperature profile retrievals derived by (i) a PC statistical regression method using high–spectral resolution AIRS infrared measurements, AMSU microwave measurements, and GPS/RO refractivity measurements, and (ii) a Bayesian estimation method using AIRS–AMSU retrieved and the operational GPS/RO temperature profiles. The operational AIRS L2 temperature products were also combined

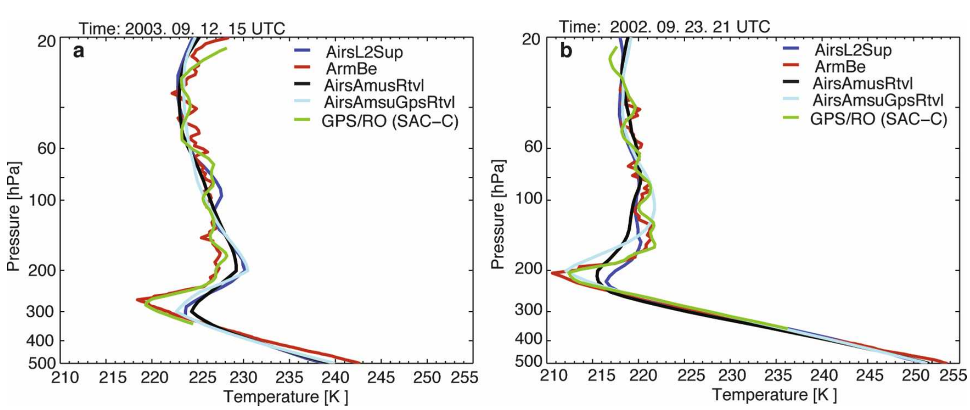

FIG. 11. Temperature profile comparisons on two different days over the NSA ARM site: (left) 12 Sep 2003 and (right) 23 Sep 2002. The red curve indicates the ARM best estimate profile (ArmBe), the black and the light blue curves represent the AIRS–AMSU PC statistical regression temperature retrieval without GPS/RO data (AirsAmsuRtvl) and with GPS/RO data (AirsAmsuGpsRtvl), respectively, and the green curve indicates the GPS/RO temperature profile [GPS/RO (SAC-C)].

with GPS/RO temperature profiles using the Bayesian estimation method. These combined retrievals were then validated with the NCEP PREPQC collocated radiosonde measurements and ARM best estimate profiles. In this study, the two methods produced very similar results.

Acknowledgments. The authors thank Paul van Delst and Hal Woolf for providing the AMSU line-by-line transmittance model code, Szuchia Moeller for processing PREPQC data, and Dave Tobin for access to the ARM site best-estimate profiles. We also thank the three anonymous reviewers for their suggestions, which improved the paper. AIRS, AMSU, PREPQC, and GPS/RO data were obtained from NASA/JPL and NCEP. This research was supported by NOAA Grant NOA07EC0676.

REFERENCES

Ackerman, S. A., K. I. Strabala, W. P. Menzel, R. A. Frey, C. C. Moeller, and L. E. Gumley, 1998: Discriminating clear-sky from clouds with MODIS. *J. Geophys. Res.,* **103,** 32 141–32 157.

Ackerman, T., and G. Stokes, 2003: The Atmospheric Radiation Measurement Program. *Phys. Today,* **56,** 38–45.

Aumann, H. H., and Coauthors, 2003: AIRS/AMSU/HSB on the Aqua mission: Design, science objectives, data products, and processing systems. *IEEE Trans. Geosci. Remote Sens.,* **41,** 253–264.

——, and Coauthors, 2005: AIRS/AMSU/HSB version 4.0 data release user guide. Jet Propulsion Laboratory, California Institute of Technology, Pasadena, CA, 72 pp. [Available online at http://daac.gsfc.nasa.gov/AIRS/documentation/v4_docs/V4_Data_Release_UG.pdf.]

Borbas, E., W. P. Menzel, J. Li, and H. M. Woolf, 2003: Combining radio occultation refractivities and IR/MW radiances to derive temperature and moisture profiles: A simulation study plus early results using CHAMP and ATOVS. *J. Geophys. Res.,* **108,** 4676, doi:10.1029/2003JD003386.

——, S. W. Seemann, H.-L. Huang, J. Li, and W. P. Menzel, 2005: Global profile training database for satellite regression retrievals with estimates of skin temperature and emissivity. *Proc. Int. TOVS Study Conf. XIV,* Beijing, China, University of Wisconsin—Madison SSEC/CIMMS, 763–770.

Collard, A. D., and S. B. Healy, 2003: The combined impact of future space-based atmospheric sounding instruments on numerical weather-prediction analysis fields: A simulation study. *Quart. J. Roy. Meteor. Soc.,* **129,** 2741–2760.

Cucurull, L., Y. Kuo, D. Barker, and S. R. Rizvi, 2006: Assessing the impact of simulated COSMIC GPS radio occultation data on weather analysis over the Antarctic: A case study. *Mon. Wea. Rev.,* **134,** 3283–3296.

Divakarla, M., C. B. Barnet, M. D. Goldberg, L. M. McMillin, E. Maddy, W. Wolf, and L. Zhow, 2006: Validation of AIRS temperature and water vapour retrievals with matched radiosonde measurements and forecasts. *J. Geophys. Res.,* **111,** D09S1, doi:10.1029/2005JD006116.

Goldberg, M. D., Y. Qu, L. M. McMillin, W. Wolf, L. Zhou, and M. Divakarla, 2003: AIRS near-real time products and algorithm in support of operational numerical weather prediction. *IEEE Trans. Geosci. Remote Sens.,* **41,** 379–389.

Hannon, S. E., L. L. Strow, and W. W. McMillan, 1996: Atmospheric infrared fast transmittance models: A comparison of two approaches. *Optical Spectroscopic Techniques and Instrumentation for Atmospheric and Space Research II,* P. B. Hays and J. Wang, Eds., International Society for Optical Engineering (SPIE Proceedings, Vol. 2830), 94–105.

Healy, S. B., and J. R. Eyre, 2000: Retrieving temperature, water vapour and surface pressure information from refractivity-index profiles derived by radio occultation: A simulation study. *Quart. J. Roy. Meteor. Soc.,* **126,** 1661–1683.

——, and J. N. Thepaut, 2006: Assimilation experiments with CHAMP GPS radio occultation measurements. *Quart. J. Roy. Meteor. Soc.,* **132** (615), 605–623.

Hofmann-Wellenhof, B., H. Lichtenegger, and J. Collins, 2004: *Global Positioning System: Theory and Practice*. 5th ed. Springer-Verlag, 382 pp.

Huang, H.-L., and P. Antonelli, 2001: Application of principal component analysis to high-resolution infrared measurement compression and retrieval. *J. Appl. Meteor.,* **40,** 365–388.

——, and Coauthors, 2004: International MODIS and AIRS Processing Package (IMAPP): A direct broadcast software package for the NASA Earth Observing System. *Bull. Amer. Meteor. Soc.,* **85,** 159–161.

Kuo, Y.-H., S. Sokolovskiy, R. Anthes, and V. Vandenberghe, 2000: Assimilation of GPS radio occultation data for numerical weather prediction. *Terr. Atmos. Oceanic Sci.,* **11,** 157–186.

Kursinski, E. R., G. A. Hajj, J. T. Schofield, R. P. Linfields, and K. R. Hardy, 1997: Observing Earth's atmosphere with radio occultation measurement using the Global Positioning System. *J. Geophys. Res.,* **102,** 23 429–23 465.

Liebe, H. J., G. A. Hufford, and M. G. Cotton, 1993: Propagation modeling of moist air and suspended water/ice particles at frequencies below 1000 GHz. *Proc. Atmospheric Propagation Effects through Natural and Man-Made Obscurants for Visible Through MM-Wave Radiation Conf.,* AGARD-CP-542, Palma de Mallorca, Spain, Advisory Group for Aerospace Research and Development, 3.1–3.10.

Liu, H., J. L. Anderson, and Y.-H. Kuo, 2007: Assimilation of GPS RO data with an ensemble filter: Importance of forecast error correlations. *Mon. Wea. Rev.,* **135,** 173–185.

Lorenc, A. C., 1986: Analysis methods for numerical weather prediction. *Quart. J. Roy. Meteor. Soc.,* **112,** 1177–1194.

Rocken, C., and Coauthors, 1997: Analysis and validation of GPS/MET data in the neutral atmosphere. *J. Geophys. Res.,* **102** (D25), 29 849–29 866.

——, Y.-H. Kuo, S. V. Sokolovskiy, and R. Anthes, 2004: The ROCSAT-3/COSMIC mission and application of GPS radio occultation data to weather and climate. *Remote Sensing Applications of the Global Positioning System,* M. Bevis, Y. Shoji, and S. Businger, Eds., International Society for Optical Engineering (SPIE Proceedings, Vol. 5661), 1–12.

Smith, W. L., and H. N. Woolf, 1976: The use of eigenvectors of statistical co-variance matrices for interpreting satellite sounding observations. *J. Atmos. Sci.,* **33,** 1127–1140.

Stokes, G. M., and S. E. Schwartz, 1994: The Atmospheric Radiation Measurement (ARM) program: Programmatic background and design of the cloud and radiation testbed. *Bull. Amer. Meteor. Soc.,* **75,** 1201–1221.

Strow, L. L., S. E. Hannon, S. De Souza-Machado, H. E. Motteler, and D. Tobin, 2003: An overview of the AIRS radiative transfer model. *IEEE Trans. Geosci. Remote Sens.,* **41,** 303–313.

Susskind, J., C. D. Barnet, and J. M. Blaisdell, 2003: Retrieval of atmospheric and surface parameters from AIRS/AMSU/HSB data in the presence of clouds. *IEEE Trans. Geosci. Remote Sens.,* **41,** 390–409.

——, ——, ——, L. Iredell, F. Keita, L. Kouvaris, G. Molnar, and M. Chahine, 2006: Accuracy of geophysical parameters derived from Atmospheric Infrared Sounder/Advanced Microwave Sounding Unit as a function of fractional cloud cover. *J. Geophys. Res.,* **111,** D09S17, doi:10.1029/2005JD006272.

Tobin, D. C., and Coauthors, 2006: Atmospheric Radiation Measurement site atmospheric state best estimates for Atmospheric Infrared Sounder temperature and water vapor retrieval validation. *J. Geophys. Res.,* **111,** D09S14, doi:10.1029/2005JD006103.

Ware, R., and Coauthors, 1996: GPS sounding of the atmosphere from low earth orbit: Preliminary results. *Bull. Amer. Meteor. Soc.,* **77,** 19–40.

Weisz, E., H.-L. Huang, J. Li, S. W. Seemann, E. E. Borbas, and L. Gumley, 2003: AIRS real-time sounding profile retrieval for IMAPP (International MODIS/AIRS Processing Package) users. *Proc. Int. TOVS Study Conf. XIII,* St. Adele, QC, Canada, University of Wisconsin—Madison SSEC/CIMMS, 323–330.

——, ——, ——, E. Borbas, K. Baggett, P. Thapliyal, and G. Li, 2007: International MODIS and AIRS Processing Package: AIRS products and applications. *J. Appl. Remote Sens.,* **1,** 013519, doi:10.1117/1.2766867.

Wu, X., J. Li, W. Zhang, and F. Wang, 2005: Atmospheric profile retrieval with AIRS data and validation at the ARM CART site. *Adv. Atmos. Sci.,* **22,** 647–657.